

Catalysis Science & Technology

Accepted Manuscript



This is an *Accepted Manuscript*, which has been through the Royal Society of Chemistry peer review process and has been accepted for publication.

Accepted Manuscripts are published online shortly after acceptance, before technical editing, formatting and proof reading. Using this free service, authors can make their results available to the community, in citable form, before we publish the edited article. We will replace this *Accepted Manuscript* with the edited and formatted *Advance Article* as soon as it is available.

You can find more information about *Accepted Manuscripts* in the [Information for Authors](#).

Please note that technical editing may introduce minor changes to the text and/or graphics, which may alter content. The journal's standard [Terms & Conditions](#) and the [Ethical guidelines](#) still apply. In no event shall the Royal Society of Chemistry be held responsible for any errors or omissions in this *Accepted Manuscript* or any consequences arising from the use of any information it contains.



Journal Name

ARTICLE

Catalytic oxidation of methyl bromide using ruthenium-based catalysts

Received 00th January 20xx,
Accepted 00th January 20xx

DOI: 10.1039/x0xx00000x

www.rsc.org/

Xiaolong Liu,^a Junlin Zeng,^{a, b} Jian Wang,^{a, c} Wenbo Shi,^{a, d} and Tingyu Zhu^{a, *}

Ruthenium-based catalysts of Ru/TiO₂, Ru/SiO₂, Ru/γ-Al₂O₃, and Ru/ZrO₂ were prepared and evaluated in CH₃Br oxidation, and Ru/TiO₂ showed better catalytic performance than other samples. The products yield and selectivity were also studied. The thermal stability was examined with a 48 h on-stream test. The influence of water vapor on the catalytic oxidation of CH₃Br was studied at 210 °C and 230 °C, and it could be found that the inhibition effect weakened with the increase of temperature. Additionally, Ru/TiO₂ was also employed in the catalytic oxidation of CO, benzene, methyl acetate, and multi-pollutants of the simulated PTA offgas.

1. Introduction

Volatile organic compounds (VOCs) emitted from industrial processes and automotive exhausts are recognized as potent contributors to the air pollution and dangerous to human health.¹⁻⁴ Among the abundant VOCs pollutants, halogenated volatile organic compounds (HVOCs) such as chlorinated volatile organic compounds (CVOCs) and brominated volatile organic compounds (BVOCs), have gained increasing attention due to their higher toxicity and difficulty to eliminate.⁵⁻⁸ The most common approaches for HVOCs removal include thermal combustion,⁹ catalytic oxidation,¹⁰⁻¹² and adsorption-based techniques,¹³ whereas catalytic oxidation has been regarded as the most promising method because of its advantages of higher efficiency and no secondary pollution.^{14, 15}

Noteworthy, catalysts for HVOCs removal basically majored in the field of CVOCs oxidation.¹⁶⁻²¹ Recently, numerous catalysts have been developed, such as noble metals²²⁻²⁶ and transition metal oxides.²⁷⁻³¹ However, platinum and palladium-containing materials tend to yield multi-chlorinated byproducts in percentage levels and be deactivated due to the Cl adsorption and the formation of oxychloride.^{32, 33} Transition metal oxides have been increasingly explored as the catalysts for oxidation of CVOCs. Nevertheless, lower activity is still the key blockage to be solved.³⁴⁻³⁶ Vanadium and chromium oxides have been established as efficient catalysts

for CVOCs oxidation,³⁷⁻⁴² while the drawback of not being environmental friendly limits their wide applications.

BVOCs are commonly emitted from the petrochemical, pharmaceutical, and other chemical processes. Typically, methyl bromide (CH₃Br) has been widely used historically as a soil fumigant and chemosterilant for durable and fresh commodities in trade channels.⁴³ In 1992, CH₃Br was listed as an ozone depleting substance under the Montreal Protocol, and phased out by 2005 in many developed countries. However, CH₃Br is still in use in most developing countries. More to the point, it is also an inevitable pollutant in the purified terephthalic acid (PTA) offgas within the range of 0~100 ppm.⁴⁴ Meanwhile, the research focused on CH₃Br elimination is far less reported.

Chen and Pignatello employed CeO₂-Al₂O₃ supported platinum catalysts to decompose methyl bromide (CH₃Br), and the complete oxidation could be realized at 400 °C.⁴³ Chen *et al* from Degussa Corporation compared the catalytic performance of platinum-based catalysts with different supports in the oxidation of simulated PTA offgas, presenting a superior self-developed washcoat support.⁴⁴ More than 80% of CH₃Br (35 ppm) and other VOCs were converted at 300 °C when the best support was used. Additionally, two catalysts of HDC 25 using above mentioned support and commercial HDC 7 with compositions unstated were also tested, and the complete oxidation of CH₃Br was realized at 270 °C and 300 °C, respectively.

Ruthenium catalysts have been well established in CO oxidation,⁴⁵⁻⁴⁷ deacon process,⁴⁸⁻⁵⁰ and catalytic oxidation of VOCs.⁵¹⁻⁵³ Complete oxidation of ethyl acetate,⁵⁴ propane,⁵⁵⁻⁵⁸ and toluene^{59, 60} could be accomplished within the temperature range of 175-275 °C. Noteworthy, Mitsui *et al* compared the catalytic performance of CeO₂ supported noble metals in oxidation of ethyl acetate, such as Ru, Pt, Pd, and Rh, respectively, and found that Ru/CeO₂ exhibited the highest catalytic activity.⁶¹ Most recently, Wang *et al* reported Ru-based materials as ideal catalysts for CVOCs abatements,⁶²⁻⁶⁵ showing less multi-chlorinated byproducts and better stability than many other catalytic systems. Hence, it is of great interest to

^a Beijing Engineering Research Center of Process Pollution Control, National Engineering Laboratory for Hydrometallurgical Cleaner Production Technology, Institute of Process Engineering, Chinese Academy of Sciences, Beijing 100190, China.

^b Chemistry and Chemical Engineering, Guizhou University, Guiyang, Guizhou 550025, China

^c Graduate University of Chinese Academy of Sciences, Beijing 100049, China

^d Institute of Chemical Engineering, China University of Petroleum, Beijing, 102249, China

E-mail address: tyzhu@ipe.ac.cn; Tel./Fax: +86-010-82544821.

† Electronic Supplementary Information (ESI) available: XPS data (Table S1), and The catalytic evaluation platform (Fig. S1). See DOI: 10.1039/x0xx00000x

explore the applicability of ruthenium materials in the oxidation of BVOCs, especially CH₃Br.

To the best of our knowledge, Ru catalyzed complete oxidation of CH₃Br has not been reported. Herein, Ru catalysts with different supports were prepared through impregnation method. Tests were conducted to explore their catalytic activities in complete oxidation of CH₃Br and simulated PTA offgas. The catalysts were characterized by BET, XRD, HRTEM, and XPS to study their chemical and physical properties, which correspond with their catalytic activities.

2. Experimental section

2.1. Catalyst preparation

Supported Ru catalysts were prepared using impregnation method with the weight percentages of Ru element being 1 wt.%. Aqueous solution of Ru(NO)(NO₃)₃ (1.5 mg/mL, Aladdin) was used as Ru resource. The following metal oxides were selected as supports: commercial P25 TiO₂ (Degussa, $S_{\text{BET}} = 57.5 \text{ m}^2/\text{g}$), SiO₂ (Aladdin, $S_{\text{BET}} = 350.2 \text{ m}^2/\text{g}$), γ -Al₂O₃ (Aladdin, $S_{\text{BET}} = 127.5 \text{ m}^2/\text{g}$), and ZrO₂ (Aladdin, $S_{\text{BET}} = 22.3 \text{ m}^2/\text{g}$). In a typical preparation, the respective support was mixed with the solution of Ru(NO)(NO₃)₃, and the mixture was stirred for 5 h at room temperature. Then the solvent was removed using a rotary evaporation, and the resulting solid was dried at 110 °C for 5 h. Subsequently, the solid was calcined in a muffle furnace at ramp of 5 °C min⁻¹ from 30 °C to 350 °C and kept at this temperature for 3 h, giving grey powder of the as-expected catalysts, which were denoted as Ru/TiO₂, Ru/SiO₂, Ru/ γ -Al₂O₃, and Ru/ZrO₂, respectively.

2.2. Catalyst characterization

Physicochemical properties of the catalysts were characterized by means of techniques. The Ru content was measured by an inductively coupled plasma-optical emission spectrometer (ICP-OES, Optima 5300DV, Perkin Elmer). X-ray diffraction (XRD) patterns of the samples were recorded on a powder diffractometer (Rigaku D/Max-RA) using Cu K α radiation (40 kV and 120 mA). The porous texture was characterized by N₂ adsorption at 77 K in an automatic surface area and porosity analyzer (Autosorb iQ, Quantachrome). Transmission electron microscopy (TEM) and High resolution transmission electron microscopy (HR-TEM) were taken on a Tecnai G2 F20 S-TWIN field emission transmission electron microscope operated at 200 kV. X-ray photoelectron spectroscopy (XPS) measurements were conducted on a Thermo escalab 250Xi X-ray using Al K α source.

TEM images of Ru/TiO₂ and pre-reduced Ru/TiO₂ samples were collected for comparison, and the pre-reduced Ru/TiO₂ sample was prepared by reduction of freshly synthesized Ru/TiO₂ sample in a 5 vol.% H₂/Ar at 450 °C for 6h. XPS spectra were collected for fresh and used Ru/TiO₂ samples.

2.3. Catalytic evaluation

Catalytic reactions were carried out in a continuous flow fixed-bed quartz microreactor (i.d. = 4 mm) from 100 to 300 °C with 100 mg of catalyst (80-100 mesh). CO, methyl bromide, benzene, and methyl acetate were introduced from the gas cylinders, and their concentrations in the total flow of the reactant mixture were calibrated by GC through a by-pass. For CO oxidation, the reaction feed was 3500 ppm CO + 20% O₂ + Ar (balance). For the oxidation of methyl bromide, benzene, or methyl acetate, the reaction feed was

VOC + 20% O₂ + Ar (balance), and their concentrations were 100, 200, and 500 ppm, respectively. Water was introduced by passage of Ar through a heated saturator. In the test of simulated PTA offgas, the concentrations of all pollutants were the same with the single pollutant test. In all catalytic experiments, the total flow ratio of the reactant mixture was 100 mL/min with the weight hourly space velocity (WHSV) of 60,000 mL/(g h). The pollutant load of F^o(MB)/W defined as the ratio of pollutant amount to the catalyst mass is calculated to be 0.00027 mol/(g h). Before the test, the sample was pretreated at 250 °C in a 20% O₂/Ar stream for 0.5 h. After the pretreatment, the reactant gas was introduced to the reactor. Analysis of the reactants and products were performed on-line with a gas chromatography (GC 2010 Plus, Shimadzu) equipped with a flame ionization detector (FID). Bromine products in the reactor effluent gases were determined via the titration method and an ion chromatography (IonPac, Dionex) according to a previous literature.⁴³ Within the temperature range of 140-160 °C, yielded Br₂ could be determined by extending the absorption time of NaOH solution used for trapping the downstream of the reactor. The conversion, Br₂ selectivity, and Br₂ yield were calculated using the following equations (1-3), respectively.

$$X = \frac{C(\text{in}) - C(\text{out})}{C(\text{in})} \times 100\% \quad (1)$$

$$\text{Br}_2 \text{ selectivity} = \frac{2 \times C(\text{Br}_2)}{C(\text{CH}_3\text{Br consumed})} \times 100\% \quad (2)$$

$$\text{Br}_2 \text{ yield} = \frac{2 \times C(\text{Br}_2)}{C(\text{CH}_3\text{Br in})} \times 100\% \quad (3)$$

where X is the conversion, $C(\text{in})$ and $C(\text{out})$ are the inlet and outlet concentration of the gaseous reactant and $C(\text{Br}_2)$ is the outlet concentration of Br₂. Besides, $C(\text{CH}_3\text{Br consumed})$ and $C(\text{CH}_3\text{Br in})$ are the consumed and the inlet concentration of CH₃Br.

3. Results and discussion

As shown in table 1, the S_{BET} of the Ru-based catalysts showed slight decrease in comparison to the original supports due to a very low Ru loading employed. It can be found that the ruthenium contents of the catalysts are very close to the calculated values of 1 wt.%. The XRD patterns of the Ru-based catalysts are shown in figure 1. The diffraction patterns of as-calcined Ru/TiO₂ and Ru/ZrO₂ were

Table 1. The BET surface areas, Ru contents, and catalytic activities of the catalysts.

Catalyst	S_{BET} (m ² /g)	Ru content (wt.%) ^a	$T_{50\%}$ (°C)	$T_{90\%}$ (°C)
Ru/TiO ₂	56.9	1.0 (1.02)	190	212
Ru/SiO ₂	348.3	1.0 (0.98)	203	223
Ru/ γ -Al ₂ O ₃	126.4	1.0 (1.01)	218	228
Ru/ZrO ₂	21.2	1.0 (1.03)	200	232

^a The data in parenthesis show the values measured by ICP-OES.

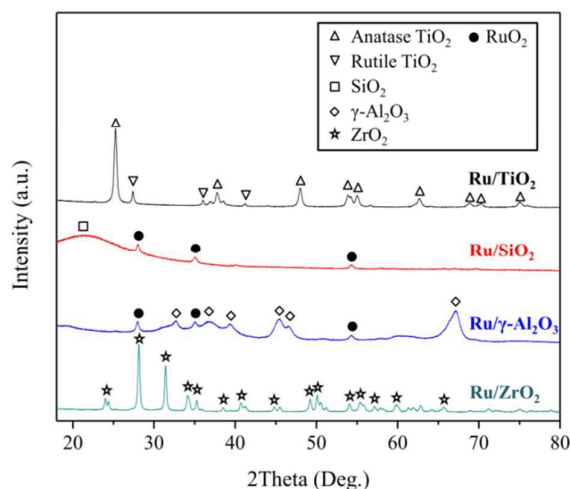


Fig. 1 XRD patterns of the Ru-based catalysts

consistent with those of unloaded TiO_2 and ZrO_2 supports, respectively, with no peaks attributable to the ruthenium species possibly due to their well-dispersion. For Ru/SiO_2 and $\text{Ru}/\gamma\text{-Al}_2\text{O}_3$, the peaks at 28.0° , 35.1° , 54.3° ascribed to RuO_2 were observed, demonstrating lower degree of ruthenium dispersion which might be caused by the aggregation of RuO_2 during the calcination.

The catalytic oxidation of CH_3Br over all catalysts were carried out under the condition of 100 ppm CH_3Br at a WHSV of 60,000 mL/(g h) within $140\sim 260^\circ\text{C}$. Representative $T_{50\%}$ (50% CH_3Br conversion corresponding to the reaction temperature) and $T_{90\%}$ of Ru/TiO_2 , Ru/SiO_2 , $\text{Ru}/\gamma\text{-Al}_2\text{O}_3$, and Ru/ZrO_2 were summarized in table 1. As illustrated in table 1 and figure 2, Ru/TiO_2 gave the lowest $T_{90\%}$ of 212°C , revealing that support plays an important role in the catalytic system. The S_{BET} of Ru/TiO_2 was far smaller than that of Ru/SiO_2 and $\text{Ru}/\gamma\text{-Al}_2\text{O}_3$, suggesting no correlation between the catalytic activity and the specific surface area. It was believed that the high activity of Ru/TiO_2 was due to the well-dispersion of Ru species based on the XRD characterizations. Besides, our latest research also showed that Ru/TiO_2 exhibited excellent thermal stability and anti-halogen poisoning properties due to strong interaction between Ru and rutile- TiO_2 from the P25 support.⁶⁶ Noteworthy, the catalytic efficiency of Ru/TiO_2 was even higher than reported platinum-containing catalysts.⁴⁴ Accordingly, Ru/TiO_2 was selected and employed in the following research.

In all catalytic tests, the Ru/TiO_2 catalysts were calcined in air and then used without any pretreatment. Considering the catalytic activity might be greatly influenced by Ru distributions, TEM characterizations were conducted to observe the morphology of ruthenium in Ru/TiO_2 . As shown in figure 3a and 3b, ruthenium species were not observed possibly due to the low contrast of ruthenium oxides. Accordingly, the pre-reduced Ru/TiO_2 was prepared only for TEM characterizations to observe the Ru distributions on the catalyst surface. The ruthenium nanoparticles (2~4 nm) decorate on the TiO_2 support, showing a heterogeneous distribution (figure 3c). HRTEM image of the marked region was collected and presented as figure 3d. The interplanar lattice spacings for anatase (001) as well as rutile (110) of TiO_2 were observed, and the ruthenium nanoparticles are mostly distributed

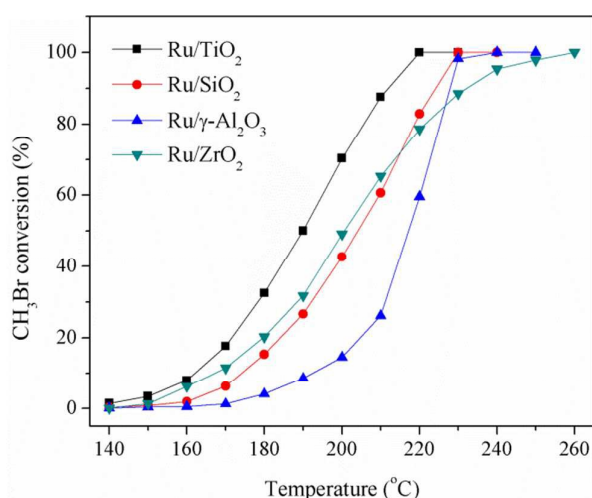


Fig. 2 CH_3Br conversion as a function of reaction temperature over the catalysts under the conditions of CH_3Br concentration = 100 ppm, $\text{CH}_3\text{Br}/\text{O}_2$ molar ratio = 1/2000, and WHSV = 60,000 mL/(g h).

on the rutile phase of P25, which is consistent with previous report.⁵⁵

In order to explore the chemical states of the ruthenium species, XPS spectra for the fresh and used Ru/TiO_2 catalysts were collected. The assignments and explanations of the Ru peaks were controversial and inconsistent in previous reports.^{67, 68} In this research (figure 4), the Ru 3d spectra were tentatively deconvoluted into three peaks at 280.1, 281.5, and 282.7 eV, which could be assigned to Ru_{CUS} (coordinatively unsaturated site), $\text{Ru}_{\text{CUS+O}_{\text{ot}}}$ (Ru_{CUS} bonded with on-top O), and $\text{Ru}^{4+}_{\text{satellite}}$ (satellite peak of bulk Ru^{4+}).^{69, 70} The Ru_{CUS} has been demonstrated as catalytically active sites, and Ru_{CUS} species dominated in the fresh and used catalyst at the ratios of 59.6% and 52.8%, revealing slight decrease during the catalytic oxidation. Besides, the Ru/Ti surface atomic ratios for the fresh and used catalysts were calculated to be 0.022 and 0.013 (table S1), respectively, illustrating a decrease of Ru dispersion.

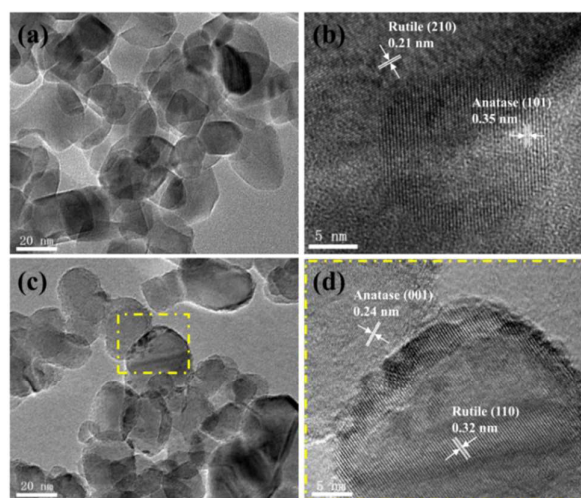


Fig. 3 TEM and HRTEM images of the catalysts: (a, b) Ru/TiO_2 , (c, d) pre-reduced Ru/TiO_2 .

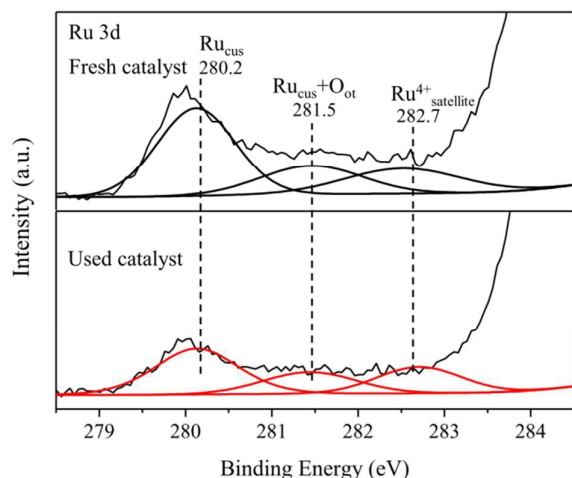


Fig. 4 XPS spectra of Ru 3d for the fresh and used Ru/TiO₂ catalysts.

In the oxidation of CH₃Br, HBr and Br₂ were produced, and their yields were mainly dependent on the reaction temperature. The possible reactions are described as below. It can be seen that reaction (5) is more thermodynamically favorable than reaction (4) at standard temperature and pressure (STP), and likely maintaining the same tendency at the higher temperatures.⁴³ It has been reported that Cl₂ was easily formed in ruthenium-catalyzed CVOCS oxidation due to the HCl Deacon reaction, where ruthenium catalyst is highly efficient.⁶⁴ Hence, we believe that Br₂ was generated either directly from the oxidation of CH₃Br or indirectly from the oxidation of HBr via the Deacon-type reaction (Eq. (6)). The HBr Deacon-type reaction is thermodynamically more favorable than HCl Deacon reaction ($\Delta G_{\text{STP}}^0 = -119$ kJ/mol for Br and -38.0 kJ/mol for Cl).⁴³ Br₂ selectivity was calculated based on the outlet concentrations of Br₂ and the consumed amount of CH₃Br. As shown in figure 5, Br₂ selectivity apparently increased from 57% to 95% with the temperature improvement. The yields of HBr and Br₂ were also obtained, and the total Br yield was basically stoichiometric to the CH₃Br consumed. Br₂ yield curve was included in figure 5, showing

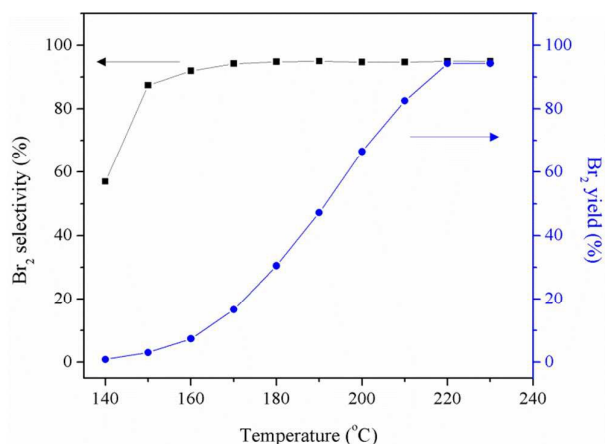


Fig. 5 Br₂ selectivity and Br₂ yield as a function of reaction temperature over Ru/TiO₂ under the conditions of CH₃Br concentration = 100 ppm, CH₃Br/O₂ molar ratio = 1/2000, and WHSV = 60,000 mL/(g h).

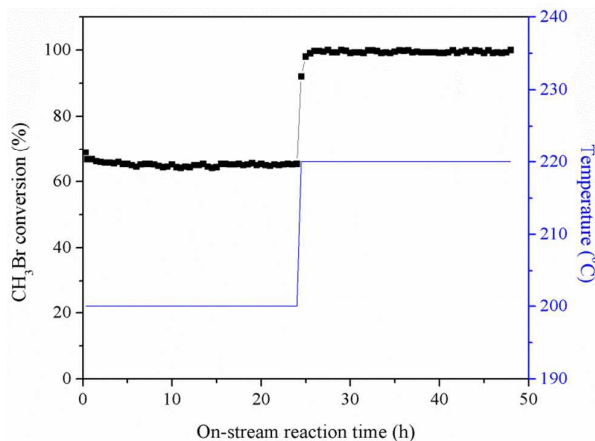
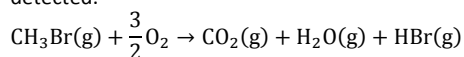
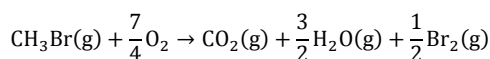


Fig. 6 CH₃Br conversion as a function of on-stream reaction time at 200 °C and 220 °C over Ru/TiO₂ under the conditions of CH₃Br concentration = 100 ppm, CH₃Br/O₂ molar ratio = 1/2000, and WHSV = 60,000 mL/(g h).

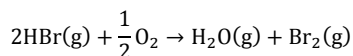
the similar tendency to CH₃Br conversion. Br₂ yield reached to 94% during the complete oxidation of CH₃Br at 220 °C. Noteworthy, CH₂Br₂ or other multi-brominated organic compounds were not detected.



$$\Delta G_{\text{STP}}^0 = -650 \text{ kJ/mol} \quad (4)$$



$$\Delta G_{\text{STP}}^0 = -709 \text{ kJ/mol} \quad (5)$$



$$\Delta G_{\text{STP}}^0 = -119 \text{ kJ/mol} \quad (6)$$

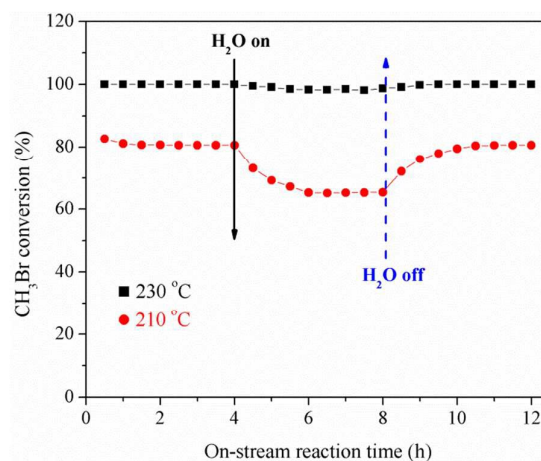


Fig. 7 Effect of water vapor on CH₃Br conversion at different temperatures over Ru/TiO₂ under the conditions of CH₃Br concentration = 100 ppm, CH₃Br/O₂ molar ratio = 1/2000, and WHSV = 60,000 mL/(g h).

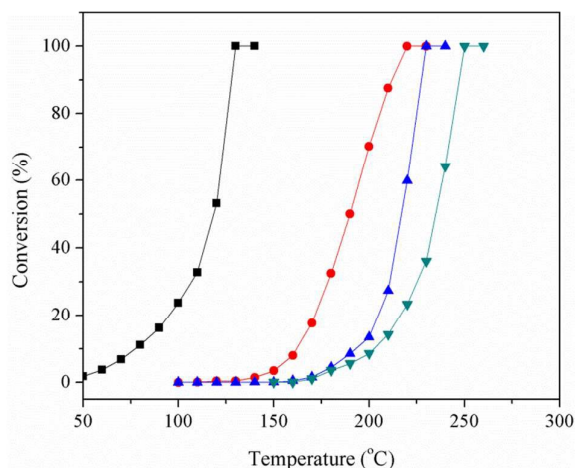


Fig. 8 Single pollutant test: CO (■), CH₃Br (●), benzene (▲), and methyl acetate (▼) conversions as a function of reaction temperature over Ru/TiO₂ under the conditions of pollutants concentrations = 3500 ppm, 100 ppm, 200 ppm, and 500 ppm, respectively, O₂ concentration = 20 vol%, and WHSV =60,000 mL/(g h).

To examine the catalytic stability, on-stream CH₃Br oxidation was performed at 200 °C and 220 °C, respectively. As shown in figure 6, CH₃Br conversion was stabilized at around 65% during the period of temperature being 200 °C. When the temperature was improved to 220 °C, a basically complete oxidation of CH₃Br was observed, and no significant decrease in catalytic activity appeared, illustrating that the Ru/TiO₂ catalyst was catalytically durable.

Water vapor commonly exists in the VOCs-containing industrial offgas with a percentage level, and the anti-moisture performance of the catalyst is an important factor to evaluate its applicability. Hence, catalytic oxidation of CH₃Br was conducted in presence of 1.5 vol% water vapor. As shown in figure 7, when the temperature was set at 210 °C, CH₃Br conversion slightly decreased from 82% to 80% within 1st h, possibly due to the unbalanced heat release. Then CH₃Br conversion was stabilized at 80%. When water vapor was introduced, apparent decrease of the conversion from 80% to 65% occurred, illustrating that water showed an inhibition effect on the catalytic process by occupying abundant active sites of the catalyst. When water vapor was cut off, the catalytic efficiency was basically recovered. For the reaction conducted at 230 °C, the introduction of water vapor barely influence the catalytic efficiency of Ru/TiO₂.

Based on above results, it can be temporarily concluded that Ru/TiO₂ was a suitable catalyst for CH₃Br oxidation. However, in the typical CH₃Br-containing emission, such as PTA offgas, abundant other pollutants including CO, BTX (benzene, toluene, and *p*-xylene), and methyl acetate exist. Hence, employment of Ru/TiO₂ in catalytic oxidation was then extended. In the single pollutant test, benzene was selected as a typical compound for BTX oxidation, and the concentrations of CO, CH₃Br, benzene, and methyl acetate were selected based on the actual PTA offgas. Complete oxidations of the pollutants were achieved at 130 °C, 220 °C, 230 °C, and 250 °C, respectively.

To examine the catalytic performance of Ru/TiO₂ in simulated PTA offgas, multi-pollutants test was then conducted. Interestingly,

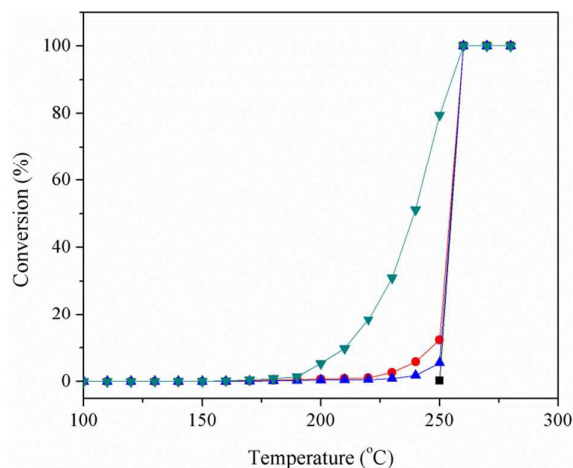


Fig. 9 Multi-pollutants test: CO (■), CH₃Br (●), benzene (▲), and methyl acetate (▼) conversions as a function of reaction temperature over Ru/TiO₂ under the conditions of pollutants concentrations = 3500 ppm, 100 ppm, 200 ppm, and 500 ppm, respectively, O₂ concentration = 20 vol%, and WHSV =60,000 mL/(g h).

when the temperature was below 200 °C, all pollutants gave the conversions below 10%, which was far different from the single pollutant test. For CO, the outlet concentration was even higher than the inlet concentration due to the oxidation of the organic pollutants into CO within the temperature range of 200-240 °C (table S2 in Supporting Information). For a better figure illustration, the CO conversion was shown in figure 9 from 250 °C. With the temperature improved, conversion of methyl acetate gently increased, showing a similar oxidation behavior to the single pollutant test. However, CO, CH₃Br and benzene still maintained at very low conversions. When the temperature was raised to 260 °C, conversions of CO, CH₃Br and benzene drastically increased to 100%, realizing a synchronous complete oxidation with methyl acetate. It was tentatively proposed that the oxygen-rich property of methyl acetate is the key factor in winning the competition oxidation with other compounds on the catalyst surface. During the oxidation, intramolecular oxygen of methyl acetate plays an important role by binding and occupying the ruthenium active sites far more easily than other compounds, and the oxidation priority was accordingly achieved. To verify our proposal, the multi-pollutants test without methyl acetate was conducted. As shown in figure S2, complete oxidation of CO, benzene and CH₃Br was achieved at 220 °C, 240 °C, and 250 °C, respectively, giving an experimental phenomenon apparently different from that of the multi-pollutants test with methyl acetate.

4. Conclusions

Ru/Support (Support = TiO₂, SiO₂, γ -Al₂O₃, and ZrO₂) samples were synthesized and employed as catalysts for CH₃Br oxidation, and Ru/TiO₂ contributed the highest catalytic activity. TEM characterizations revealed that ruthenium species mainly distributed on the rutile phase of P25 TiO₂. In Ru/TiO₂ catalyzed CH₃Br oxidation, Br₂ was the major bromine product with the

selectivity of ca. 95% when the temperature was above 160 °C. In the on-stream reaction test, excellent thermal stability and anti-bromine property have been well demonstrated for Ru/TiO₂. Water vapor showed an inhibition effect for CH₃Br oxidation at 210 °C, whereas the inhibition greatly weakened at a relatively higher temperature of 230 °C, and CH₃Br conversion basically maintained at 100%, demonstrating a great anti-moisture performance. Additionally, Ru/TiO₂ also showed great catalytic efficiency for CO, benzene, and methyl acetate. In the test of simulated PTA offgas with multi-pollutants, apparent competitive oxidation was observed, and a synchronously complete oxidation was achieved.

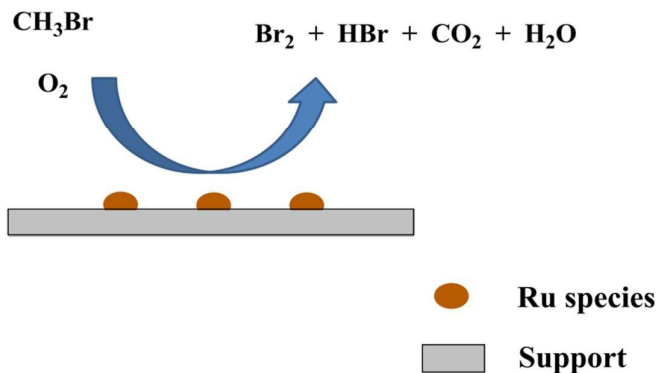
Acknowledgements

This work was supported by the Strategic Priority Research Program of the Chinese Academy of Sciences (No. XDB05050100) and the National Natural Science Foundation of China (No. 21207132).

Notes and references

- J. I. Gutiérrez-Ortiz, B. de Rivas, R. López-Fonseca and J. R. González-Velasco, *Appl. Catal., B*, 2006, **65**, 191-200.
- M. Ousmane, L. F. Liotta, G. Di Carlo, G. Pantaleo, A. M. Venezia, G. Deganello, L. Retaillieu, A. Boreave and A. Giroir-Fendler, *Appl. Catal., B*, 2011, **101**, 629-637.
- L. F. Liotta, H. Wu, G. Pantaleo and A. M. Venezia, *Catal. Sci. Technol.*, 2013, **3**, 3085-3102.
- S. Xia, H. Zhu, H. Cai, J. Zhang, J. Yu and Z. Tang, *Rsc Adv.*, 2014, **4**, 57975-57982.
- J. Gan, N. E. Megonnell and S. R. Yates, *Atmos. Environ.*, 2001, **35**, 941-947.
- R. Delaigle, D. P. Debecker, F. Bertinchamps and E. M. Gaigneaux, *Top Catal.*, 2009, **52**, 501-516.
- B. Huang, C. Lei, C. Wei and G. Zeng, *Environ. Int.*, 2014, **71**, 118-138.
- B. Liu, X. Li, Q. Zhao, J. Liu, S. Liu, S. Wang and M. Tadé, *J. Mater. Chem. A*, 2015, **3**, 15163-15170.
- J. R. Hart, *Chemosphere*, 2004, **54**, 1539-1547.
- G. R. Lester, *Catal. Today*, 1999, **53**, 407-418.
- K. Everaert and J. Baeyens, *J. Hazard. Mater.*, 2004, **109**, 113-139.
- A. Aranzabal, B. Pereda-Ayo, M. P. González-Marcos, J. A. González-Marcos, R. López-Fonseca and J. R. González-Velasco, *Chem. Pap.*, 2014, **68**, 1169-1186.
- J. Lemus, M. Martin-Martinez, J. Palomar, L. Gomez-Sainero, M. A. Gilarranz and J. J. Rodriguez, *Chem. Eng. J.*, 2012, **211**, 246-254.
- S. Ojala, S. Pitkääho, T. Laitinen, N. N. Koivikko, R. Brahmī, J. Gaálová, L. Matejova, A. Kucherov, S. Päiväranta, C. Hirschmann, T. Nevanperä, M. Riihimäki, M. Piriä and R. L. Keiski, *Top Catal.*, 2011, **54**, 1224-1256.
- H. Huang, Y. Xu, Q. Feng and D. Y. C. Leung, *Catal. Sci. Technol.*, 2015, **5**, 2649-2669.
- A. Musialik-Piotrowska and K. Syczewska, *Catal. Today*, 2002, **73**, 333-342.
- S. Lomnicki, J. Lichtenberger, Z. T. Xu, M. Waters, J. Kosman and M. D. Amiridis, *Appl. Catal., B*, 2003, **46**, 105-119.
- D. P. Debecker, F. Bertinchamps, N. Blangenois, P. Eloy and E. M. Gaigneaux, *Appl. Catal., B*, 2007, **74**, 223-232.
- S. Pitkääho, S. Ojala, T. Kinnunen, R. Silvonen and R. L. Keiski, *Top Catal*, 2011, **54**, 1257-1265.
- S. Pitkääho, S. Ojala, T. Maunula, A. Savimäki, T. Kinnunen and R. L. Keiski, *Appl. Catal., B*, 2011, **102**, 395-403.
- P. Topka, R. Delaigle, L. Kaluža and E. M. Gaigneaux, *Catal. Today*, 2015, **253**, 172-177.
- J. R. González-Velasco, A. Aranzabal, J. I. Gutiérrez-Ortiz, R. López-Fonseca and M. A. Gutiérrez-Ortiz, *Appl. Catal., B*, 1998, **19**, 189-197.
- R. López-Fonseca, J. I. Gutiérrez-Ortiz, M. A. Gutiérrez-Ortiz and J. R. González-Velasco, *Catal. Today*, 2005, **107-108**, 200-207.
- S. Scirè and L. F. Liotta, *Appl. Catal., B*, 2012, **125**, 222-246.
- L. Matějová, P. Topka, L. Kaluža, S. Pitkääho, S. Ojala, J. Gaálová and R. L. Keiski, *Appl. Catal., B*, 2013, **142**, 54-64.
- S. Pitkääho, T. Nevanperä, L. Matejova, S. Ojala and R. L. Keiski, *Appl. Catal., B*, 2013, **138**, 33-42.
- A. Z. Abdullah, M. Z. Abu Bakar and S. Bhatia, *J. Hazard. Mater.*, 2006, **129**, 39-49.
- F. Bertinchamps, C. Poleunis, C. Gregoire, P. Eloy, P. Bertrand and E. M. Gaigneaux, *Surf. Interface Anal.*, 2008, **40**, 231-236.
- D. P. Debecker, R. Delaigle, K. Bouchmella, P. Eloy, E. M. Gaigneaux and P. H. Mutin, *Catal. Today*, 2010, **157**, 125-130.
- T. K. Tseng, L. Wang, C. T. Ho and H. Chu, *J. Hazard. Mater.*, 2010, **178**, 1035-1040.
- J. Wang, X. Wang, X. Liu, T. Zhu, Y. Guo and H. Qi, *Catal. Today*, 2015, **241**, 92-99.
- R. W. van den Brink, R. Louw and P. Mulder, *Appl. Catal., B*, 1998, **16**, 219-226.
- L. F. Liotta, *Appl. Catal., B*, 2010, **100**, 403-412.
- F. Bertinchamps, C. Grágoire and E. M. Gaigneaux, *Appl. Catal., B*, 2006, **66**, 10-22.
- F. Bertinchamps, C. Grágoire and E. M. Gaigneaux, *Appl. Catal., B*, 2006, **66**, 1-9.
- B. de Rivas, R. López-Fonseca, C. Jiménez-González and J. I. Gutiérrez-Ortiz, *J. Catal.*, 2011, **281**, 88-97.
- S. Krishnamoorthy, J. A. Rivas and M. D. Amiridis, *J. Catal.*, 2000, **193**, 264-272.
- J. Lichtenberger and M. D. Amiridis, *J. Catal.*, 2004, **223**, 296-308.
- D. P. Debecker, R. Delaigle, P. Eloy and E. M. Gaigneaux, *J. Mol. Catal. A-Chem.*, 2008, **289**, 38-43.
- C. E. Hetrick, J. Lichtenberger and M. D. Amiridis, *Appl. Catal., B*, 2008, **77**, 255-263.
- C. E. Hetrick, F. Patcas and M. D. Amiridis, *Appl. Catal., B*, 2011, **101**, 622-628.
- P. Yang, S. Yang, Z. Shi, Z. Meng and R. Zhou, *Appl. Catal., B*, 2015, **162**, 227-235.
- C. Y. Chen and J. J. Pignatello, *Appl. Catal., B*, 2013, **142**, 785-794.
- B. Chen, J. Carson, J. Gibson, R. Renneke, T. Tacke, M. Reisinger, R. Hausmann, A. Geisselmann, G. Stochniol, and P. Panster, *Chem. Industries*, 2003, 179-190.
- F. Gao and D. W. Goodman, *Phys. Chem. Chem. Phys.*, 2012, **14**, 6688-6697.
- K. Qadir, S. H. Joo, B. S. Mun, D. R. Butcher, J. R. Renzas, F. Aksoy, Z. Liu, G. A. Somorjai and J. Y. Park, *Nano Lett.*, 2012, **12**, 5761-5768.
- H. Öström, H. Öberg, H. Xin, J. LaRue, M. Beye, M. Dell'Angela, J. Gladh, M. L. Ng, J. A. Sellberg, S. Kaya, G. Mercurio, D. Nordlund, M. Hantschmann, F. Hieke, D. Kuhn, W. F. Schlotter, G. L. Dakovski, J. J. Turner, M. P. Minitti, A. Mitra, S. P. Moeller, A. Fohlisch, M. Wolf, W. Wurth, M. Persson, J. K. Nørskov, F. Abild-Pedersen, H. Ogasawara, L. G. M. Pettersson and A. Nilsson, *Science*, 2015, **347**, 978-982.
- N. López, J. Gómez-Segura, R. P. Marín and J. Pérez-Ramírez, *J. Catal.*, 2008, **255**, 29-39.
- C. Mondelli, A. P. Amrute, F. Krumeich, T. Schmidt and J. Perez-Ramirez, *Chemcatchem*, 2011, **3**, 657-660.
- G. Xiang, X. Shi, Y. Wu, J. Zhuang and X. Wang, *Sci. Rep.*, 2012, **2**, 801.
- T. Mitsui, K. Tsutsui, T. Matsui, R. Kikuchi and K. Eguchi, *Appl. Catal., B*, 2008, **81**, 56-63.

52. S. Aouad, E. Abi-Aad and A. Aboukaïs, *Appl. Catal., B*, 2009, **88**, 249-256.
53. J. Okal and M. Zawadzki, *Appl. Catal., B*, 2009, **89**, 22-32.
54. N. Kamiuchi, T. Mitsui, H. Muroyama, T. Matsui, R. Kikuchi and K. Eguchi, *Appl. Catal., B*, 2010, **97**, 120-126.
55. D. P. Debecker, B. Farin, E. M. Gaigneaux, C. Sanchez and C. Sassoie, *Appl. Catal. A*, 2014, **481**, 11-18.
56. J. Okal and M. Zawadzki, *Catal. Lett.*, 2009, **132**, 225-234.
57. J. Okal and M. Zawadzki, *Appl. Catal., B*, 2011, **105**, 182-190.
58. J. Okal, M. Zawadzki and W. Tylus, *Appl. Catal., B*, 2011, **101**, 548-559.
59. S. Aouad, E. Saab, E. Abi-Aad and A. Aboukaïs, *Kinet. Catal*, 2007, **48**, 835-840.
60. X. Liu, J. Wang, J. Zeng, X. Wang and T. Zhu, *Rsc Adv.*, 2015, **5**, 52066-52071.
61. T. Mitsui, T. Matsui, R. Kikuchi and K. Eguchi, *Top Catal.*, 2009, **52**, 464-469.
62. Q. Dai, S. Bai, Z. Wang, X. Wang and G. Lu, *Appl. Catal., B*, 2012, **126**, 64-75.
63. Q. Dai, S. Bai, J. Wang, M. Li, X. Wang and G. Lu, *Appl. Catal., B*, 2013, **142**, 222-233.
64. Q. Dai, S. Bai, X. Wang and G. Lu, *Appl. Catal., B*, 2013, **129**, 580-588.
65. H. Huang, Q. Dai and X. Wang, *Appl. Catal., B*, 2014, **158**, 96-105.
66. J. Wang, X. Liu, J. Zeng and T. Zhu, *Catal. Commu.*, 2016, **76**, 13-18.
67. H.J. Lewerenz, S. Stucki, R. Kotz, *Surf. Sci.*, 1983, **126**, 893.
68. P.A. Cox, J.B. Goodenough, P.J. Tavener, D. Telles, R.G. Egdell, *J. Solid State Chem.*, 1986, **62**, 360.
69. H. Over, A. P. Seitsonen, E. Lundgren, M. Smedh and J. N. Andersen, *Surf. Sci.*, 2002, **504**, L196-L200.
70. H. Over, A.P. Seitsonen, E. Lundgren, M. Wiklund, J.N. Andersen, *Chem. Phys. Lett.*, 2001, **342**, 467.



Ruthenium-based catalysts of Ru/TiO₂, Ru/SiO₂, Ru/ γ -Al₂O₃, and Ru/ZrO₂ were prepared and evaluated in CH₃Br oxidation, and Ru/TiO₂ showed better catalytic performance than other samples. The products selectivity, thermal stability, and anti-moisture properties were also studied. Additionally, Ru/TiO₂ was also employed in the catalytic oxidation of CO, benzene, methyl acetate, and multi-pollutants of the simulated PTA offgas.